energies

MDPI

Article

Effect of Methyl Orange Dye Concentration on Decolorization and Bioelectricity Generation in an Earthen Membrane Cylindrical Microbial Fuel Cell Reactor

Anupama Chacko [1], Narnepati Krishna Chaitanya [2], Vyshnavi Shaji [3], Pritha Chatterjee [3,4,*], Sobhanam Padmini Shibin [5], Md Tabish Noori [6,*] and P. P. Rajesh [1,*]

[1] Department of Biotechnology, Cochin University of Science and Technology, Kochi 682022, India; anupamachacko@cusat.ac.in
[2] Department of Civil Engineering, National Institute of Technology Thiruchirappalli (NIT Trichy), Tiruchirappalli 620015, India; krishna.chaitanya@cleanz.coe.iith.ac.in
[3] Department of Civil Engineerig, Indian Institute of Technology Hyderabad, Kandi, Sangareddy 502285, India; ce25resch11001@iith.ac.in
[4] Department of Climate Change, Indian Institute of Technology Hyderabad, Kandi, Sangareddy 502285, India
[5] National Centre for Aquatic Animal Health, Cochin University of Science and Technology, Kochi 682016, India; shibinsp@cusat.ac.in
[6] BIOMA Institute, University of Navarra, 31008 Pamplona, Spain
* Correspondence: pritha@ce.iith.ac.in (P.C.); tnoori@unav.es (M.T.N.); rajeshpp@cusat.ac.in (P.P.R.)

Abstract

Microbial fuel cells (MFCs) offer a sustainable approach for simultaneous azo dye removal and bioelectricity generation from wastewater. In this study, we evaluated the effect of methyl orange (MO) dye concentration on the performance of a cylindrical earthen-membrane MFC under long-term operation. Five MFC configurations, in duplicate, were operated with acetate-fed anodes for 22 operational cycles with dye concentrations ranging from 20 to 100 mg L^{-1}. Throughout the study, stable decolorization was observed with maximum dye removal efficiencies of 90.0%, 88.1%, 87.8%, 86.9%, and 86.0% at 20, 40, 60, 80, and 100 mg L^{-1} MO, respectively. The highest power density obtained was 48 mW m^{-2} for an MO concentration of 60 mg L^{-1}. Reduced power generation at higher dye concentrations (>60 mg L^{-1}) may be due to inhibitory effects on microbial electron transfer. Considering decolorization, power output, and coulombic efficiency together, 60 mg L^{-1} was identified as the optimal MO concentration, whereas up to 100 mg L^{-1} could still be decolorized by >85% at the cost of lower power output. The results indicate that low-cost earthen-membrane cylindrical MFCs are a promising technology for sustainable wastewater treatment and can effectively decolorize MO while recovering bioenergy during prolonged operation.

Keywords: bioelectrochemical systems; azo dye decolorization; exoelectrogenic bacteria; wastewater treatment; electron transfer

Check for updates

Academic Editor: Marcin Dębowski

Received: 24 September 2026
Revised: 24 October 2026
Accepted: 26 October 2026
Published: 28 October 2026

Copyright: © 2026 by the authors. Licensee MDPI, Basel, Switzerland. This article is an open access article distributed under the terms and conditions of the Creative Commons Attribution (CC BY) license.

1. Introduction

Microbial fuel cells (MFCs) are bioelectrochemical systems that generate electricity through microbial catalysis while simultaneously treating wastewater. In these systems, exoelectrogenic microorganisms oxidize biodegradable organic matter and transfer electrons to the anode, converting chemical energy into electrical energy [1]. These cost-effective, renewable, low-carbon-impact systems integrate pollutant removal with energy recovery and offer an environmentally friendly alternative to conventional wastewater treatment technologies [2]. Beyond removing biodegradable organic matter, MFCs are increasingly being

explored to treat recalcitrant pollutants, including synthetic dyes, antibiotics, pharmaceuticals, pesticides, phenolic compounds, and other industrial contaminants that conventional biological processes struggle to remove [3].

Among recalcitrant pollutants, synthetic dyes pose a major environmental concern because of their extensive industrial use and persistence. Because they are low-cost and easy to produce, synthetic dyes are widely used in the textile, printing, leather, cosmetic, food, and pharmaceutical industries [4]. The rapid growth of these industries has resulted in the continuous discharge of dye-containing wastewater into natural water bodies, adversely affecting water quality and aquatic ecosystems [5]. About 60–70% of global dye production is azo dyes, characterized by one or more azo bonds (-N=N-) linked to aromatic rings [6]. These are particularly problematic because of their structural stability and resistance to biodegradation [7], and reductive cleavage of azo bonds generates aromatic amines that are toxic, mutagenic, and potentially carcinogenic [8]. Among azo dyes, methyl orange (MO) is a widely used anionic dye frequently detected in industrial effluents and laboratory wastewater because of its extensive use as a colorant and pH indicator. Furthermore, approximately 10–15% of the applied dye remains unbound and enters wastewater streams, increasing the treatment burden [9]; even at low concentrations, dye-contaminated wastewater reduces light penetration, inhibits photosynthesis, and harms aquatic ecosystems. Consequently, there is a pressing need for an alternative treatment technology that can efficiently decolorize dyes with low energy consumption and minimal secondary pollution. In this context, MFCs offer a promising alternative because they couple microbial oxidation of organic substrates with reductive dye transformation through bioelectrochemical electron transfer.

In these systems, azo dye molecules can function as terminal electron acceptors and undergo reductive cleavage of azo bonds, leading to decolorization and detoxification [5]. This bioelectrochemical process enables efficient contaminant removal with lower aeration demand, reduced sludge generation, and partial energy recovery compared with conventional aerobic treatment systems.

Previous studies have demonstrated MFCs' potential for efficient decolorization while recovering bioelectricity. Wang et al. [10] achieved 89% decolorization of reactive blue 19 (50 mg L^{-1}) within 48 h. Improved decolorization was accompanied by enhanced electron transfer and significant shifts in the electroactive microbial community. Similarly, Agrahari et al. [11] reported decolorization efficiencies of 98.5%, 95%, and 84.5% for Reactive Black 5, Reactive Red 120, and Coomassie Brilliant Blue, respectively, using a 300 mL H-type MFC inoculated with *Pseudomonas gessardii*. In addition, the system achieved a maximum power density of 474 mW m^{-2} and nearly 70% COD removal efficiency, highlighting MFCs' ability to integrate wastewater treatment with energy recovery.

Recent research has increasingly focused on degrading MO dyes through microbial consortium engineering and advanced electrode modification to improve extracellular electron transfer. Bartolome and Tayo [12] investigated a double-chamber MFC inoculated with mixed soil microorganisms for MO decolorization. The reactor using carbon fiber brush electrodes achieved 78.1% MO removal within 10 h with a power density of 0.34 W m^{-2}, whereas titanium mesh electrodes produced a higher power density (1.22 W m^{-2}) but showed lower decolorization efficiency (61.1%), demonstrating the importance of electrode configuration on dye removal and bioelectricity production. Later, Naaz et al. [13] used a co-culture of Escherichia coli and Pseudomonas aeruginosa to enhance MO biodegradation. The reactor achieved approximately 98% decolorization of 250 mg L^{-1} MO within 48 h. They further modified the anode with Fe_2O_3 nanoparticles and observed that this modification increased the maximum power density from 6.5 to 11.2 W m^{-3} [13]. This highlights the importance of electrode engineering to enhance extracellular electron transfer. More recently, Guo et al. [14] developed a tea polyphenol-functionalized reduced graphene oxide anode

that significantly improved anode hydrophilicity and microbial attachment. The modified MFC achieved 99% MO decolorization (50 mg L^{-1}) within 48 h with a maximum power density of 773.9 mW m^{-2}, representing a 22% increase over the unmodified carbon cloth electrode. These studies demonstrate that improving extracellular electron transfer through microbial and electrode engineering substantially enhances reactor performance.

Despite these advances, several challenges continue to limit the practical application of MFCs for wastewater treatment. Dye concentration, electrode materials, inoculum source, and reactor configuration strongly influence reactor performance. Higher dye concentrations often divert electrons toward azo dye reduction rather than electricity generation, reducing coulombic efficiency and power output [5,15]. In addition, methanogenesis in mixed anaerobic inocula competes with exoelectrogenic microorganisms for available substrates, further reducing electrical performance. To mitigate methanogenic competition, Chacko et al. [16] evaluated heat pretreatment of mixed anaerobic sludge in earthen membrane cylindrical MFCs treating 25 mg L^{-1} MO dye with acetate (3 g L^{-1}) as a carbon source. Heat pretreatment effectively suppressed methanogens, resulting in complete dye removal within 4 h and a maximum power density of 134 mW m^{-2}, and improved coulombic efficiency compared with untreated inoculum. Although this study demonstrated the importance of inoculum pretreatment, the investigation was limited to a single MO concentration and short-term operation.

In practice, textile wastewater dye concentrations vary significantly depending on manufacturing process, dye formulation, and wastewater composition, leading to substantial variations in treatment performance. Therefore, understanding how increasing dye concentrations affect MFC operation is essential for assessing the feasibility of these systems under realistic conditions. Nevertheless, systematic studies evaluating the effect of increasing MO concentration on long-term MFC performance remain limited. The effects of dye loading on anodic microbial acclimation, COD removal, coulombic efficiency, substrate utilization, and stable electricity generation in low-cost earthen membrane cylindrical reactors have not been comprehensively investigated. Most previous studies have focused primarily on improving electrode materials, catalysts, or reactor configurations, whereas reactor performance across a range of dye concentrations during prolonged operation has received comparatively little attention.

It is hypothesized that the incorporation of Methyl Orange (MO) into the anodic chamber will serve as an effective electron acceptor, resulting in simultaneous high-efficiency azo dye decolorization and enhanced power density generation. Specifically, varying the MO concentration is expected to have a non-linear effect on decolorization in which increasing the initial MO concentration up to an optimal threshold will accelerate electron transfer kinetics, thereby increasing current output, beyond which increased concentrations will reduce overall system performance and prolong the time required for complete decolorization.

Therefore, this study investigates how increasing MO concentrations affect the long-term performance of earthen membrane cylindrical MFCs to determine the maximum dye loading that can be effectively treated while maintaining feasible bioelectricity generation. Five MFC configurations, each run in duplicate, were operated with acetate-fed anodes at methyl orange concentrations ranging from 20 to 100 mg L^{-1}. The study systematically evaluated dye decolorization, COD removal efficiency, coulombic efficiency, and bioelectricity generation under varying dye loadings. In addition, the work aimed to assess the stability and adaptation of anodic microbial communities during prolonged operation. The findings provide valuable insight into electron utilization and reactor performance under varying dye concentrations, thereby providing practical guidance for the application of low-cost MFCs in treating dye-containing industrial wastewater.

2. Materials and Methods

2.1. Microbial Fuel Cell Reactor Configuration and Inoculum

Dual-chamber aqueous-cathode MFCs were used in the present study. Each MFC consisted of a cathode chamber constructed using acrylic sheets and an anode chamber made of cylindrical clayware. The clayware (4 mm thick) also acts as a ceramic, ion-permeable separator. The anodic chamber of the MFC reactors had a working volume of 150 mL (excluding headspace). Carbon felt was used for both electrodes; the anode had a surface area of 99 cm^2, whereas the cathode had an area of 218 cm^2. Both the electrodes were separately woven with stainless steel wire and connected to an external resistor having a resistance of 100 Ω. The cathode chamber was filled with tap water and continuously aerated. A schematic of the reactor configuration is shown in Figure 1.

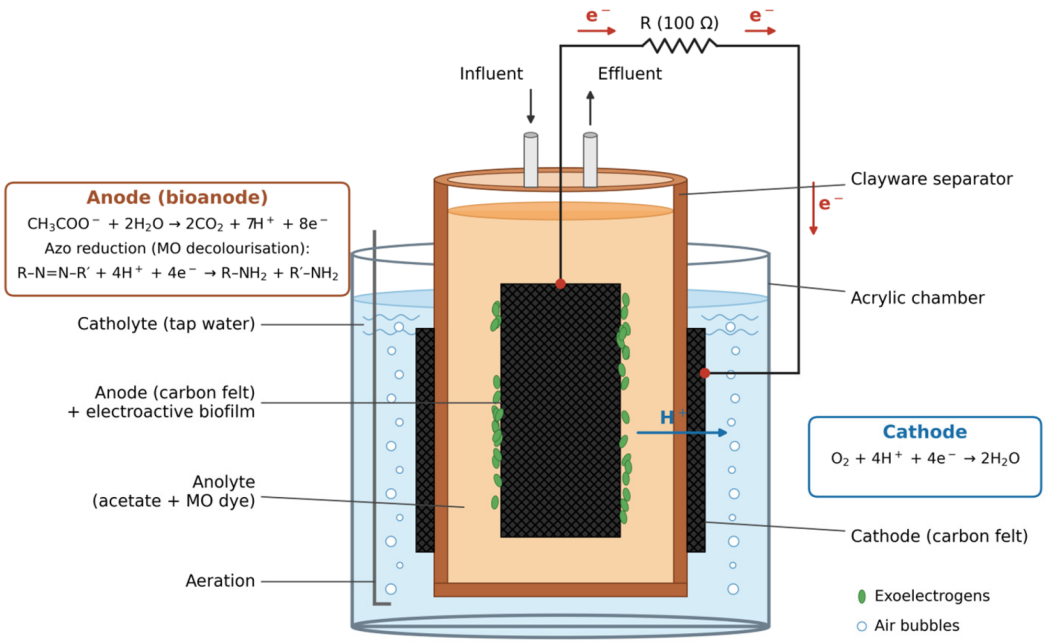


Figure 1. Schematic of the earthen membrane cylindrical MFC showing the clayware anode chamber with the carbon felt bioanode; the carbon felt cathode wrapped on the outer clayware surface in an aerated tap-water catholyte; and the principal anodic, cathodic, and azo-reduction reactions.

Twenty percent of the anode working volume was inoculated with an anaerobic sludge collected from the wastewater treatment plant of a cotton textile industry, which served as the inoculum. The inoculum was heat-pretreated at 100 °C for 15 min before use in the MFC [16]. The remaining volume was filled with MO dye-containing acetate synthetic wastewater with a COD of 3000 mg L^{-1}, as described in a previous study [16]. The acetate medium was prepared by dissolving sodium acetate, 3.84 g L^{-1} $NaHCO_3$, 4.5 g L^{-1} NH_4Cl, and 0.954 g L^{-1} $CaCl_2 \cdot 2H_2O \cdot 2H_2O$, 0.75 g L^{-1} $MgSO_4 \cdot 7H_2O$, 0.192 g L^{-1} K_2HPO_4, 0.081 g L^{-1} KH_2PO_4, and 0.027 g L^{-1} $FeSO_4 \cdot 7H_2O$ in distilled water, along with 1 mL trace element solution. The trace metal solution consists of $FeSO_4 \cdot 6H_2O$, 10.00 mg L^{-1}; $MnSO_4$, 0.526 mg L^{-1}; $ZnSO_4 \cdot 7H_2O$, 0.106 mg L^{-1}; H_3BO_3, 0.106 mg L^{-1}; and $CuSO_4 \cdot 5H_2O$, 4.5 µg L^{-1}. The media pH was 7.9–8.1, slightly alkaline. These MFCs were operated in batch mode with a 4-day feeding interval at a controlled temperature of 30–35 °C, retaining biofilm between cycles.

2.2. Effect of Varying Methyl Orange Dye Concentrations

The study aimed to determine the optimum methyl orange (MO) dye concentration for maximum decolorization with adequate current generation in laboratory-scale MFCs.

In order to evaluate the effect of different dye concentrations, identical reactors were constructed and operated for each MO dye concentration, which were designated as MFC-1 (20 mg L^{-1}), MFC-2 (40 mg L^{-1}), MFC-3 (60 mg L^{-1}), MFC-4 (80 mg L^{-1}), and MFC-5 (100 mg L^{-1}). Each dye concentration was added to separate MFCs along with synthetic wastewater. All MFCs were operated independently under the same set of conditions except dye concentration. All experiments evaluating the effect of Methyl Orange (MO) dye concentrations on MFC performance were performed in duplicate. For each reactor, samples and voltage measurements were recorded repeatedly over time. The performance of each MFC was evaluated through electrochemical and decolorization analyses.

2.3. Electrochemical Analysis and Calculations

The voltage of each MFC was measured daily using a digital multimeter (Fluke Corporation, Everett, WA, USA). The current (I) was calculated from the voltage across the external resistor using Ohm's law ($I = V/R_{ext}$). The power (P) was calculated using the equation $P = V \times I$, where P is power (W), V is voltage (V), and I is current (A). In order to find the maximum power density, current density, and internal resistance of the system, a polarization study was conducted by varying the external resistance from 10,000 Ω to 5 Ω once, at the end of the operating period (cycle 22), when the cell voltage was stable. The test started the day after anolyte replacement, and the voltage at each external resistance was recorded only after it stabilized. The polarization curve was plotted by taking current density on the *x*-axis and power density and voltage on the *y*-axis. Internal resistance was determined from the slope of the voltage versus current curve. Power and current densities were normalized to the projected anode surface area (99 cm^2). The power produced during routine operation at 100 Ω was distinguished from the maximum power density obtained from the polarization curves.

The electrochemical behavior of MFCs operated at different dye concentrations was evaluated using cyclic voltammetry (CV) and linear sweep voltammetry (LSV) (CHI potentiostat, CH Instruments, Inc., Austin, TX, USA). The voltammetric analysis was performed at a slow scan rate of 10 mV/s over a potential ranging from −1 to +1 V vs. Ag/AgCl. A three-electrode half-cell system was used for the experiment, where the anode served as a working electrode, the cathode as a counter electrode, and the Ag/AgCl electrode as the reference. CV and LSV were performed once, at the end of the operating period, in situ in each reactor, with the Ag/AgCl reference electrode placed in the anode chamber. The currents are reported in amperes as recorded by the potentiostat and were not normalized to electrode areas.

2.4. Wastewater Treatment and Coulombic Efficiency

The Chemical Oxygen Demand (COD) removal efficiency and Coulombic Efficiency (CE) of MFCs were also studied. The variation in COD removal with different MO dye concentrations was analyzed using the closed reflux titration method, following standard protocols [17]. COD removal was performed over four cycles. The initial COD of the influent was maintained at approximately 3000 mg L^{-1}, and the final COD after treatment was measured to assess removal efficiency. COD removal efficiency (%) was calculated using the following equation:

$$\text{COD removal efficiency (\%)} = \frac{COD_i - COD_f}{COD_i} \times 100 \quad (1)$$

where COD_i and COD_f represent the initial and final COD values, respectively.

The maximum coulombic efficiencies of different MFCs were calculated using the equation reported by Logan et al. [18]. The rate of charge transfer between the electrodes with respect to the change in COD in this set of MFCs was estimated by Equation (2).

$$\text{CE } (\%) = \frac{M_s \times \int_0^t I\, dt}{\text{F} \times \text{b} \times V_{an} \times \Delta\text{COD}} \times 100 \quad (2)$$

where M_s is the molecular weight of oxygen, I is the current, F is Faraday's constant, b is the number of electrons exchanged per mole of O_2 (4), V_{an} is the volume of the anodic chamber, and ΔCOD is the change in COD over time 't'.

2.5. Dye Decolorization Efficiency

Dye decolorization was monitored by measuring changes in absorbance of MO using a UV-Vis spectrophotometer (Shimadzu, Japan). Approximately 1 mL of anolyte was withdrawn from each reactor at 1 h intervals during operation. The samples were centrifuged (4000 rpm) to remove suspended particles before analysis. Absorbance was recorded at 465 nm, corresponding to the characteristic peak of MO dye. Synthetic wastewater without dye was used as the blank. The extent of decolorization was determined from the decrease in absorbance using Equation (3):

$$\text{Decolorization } (\%) = \frac{A_0 - A_t}{A_0} \times 100 \quad (3)$$

where A_0 and A_t denote the initial and final absorbance values, respectively.

2.6. Phytotoxicity Analysis

The effect of different dye concentrations on plant growth before and after MFC treatment was studied. The phytotoxicity analysis was performed using rapidly germinating *Pisum sativum* seeds. Analysis was performed for each concentration of dye, and untreated samples were also kept to check the intensity of toxicity. About ten seeds were placed in a Petri dish lined with double-layered tissue paper. Distilled water was added as a positive control, and synthetic wastewater without dye served as a negative control. The germination of each seed in every plate was observed. Root and shoot growth were observed and measured daily. The seed germination rate was then calculated.

2.7. Statistical Analysis

Each MO concentration was tested in two independently operated duplicate reactors, which were the independent experimental units. All experimental configurations were evaluated in independent duplicate blocks, designated as D1 and D2. To account for the repeated-measures structure of the longitudinal data and avoid pseudoreplication, we aggregated measurements across the 22 operational cycles into a single overall mean value for each reactor run. Statistical processing was executed using Microsoft Excel via the Analysis ToolPak. Variations in Coulombic efficiency and sustainable power density across the distinct operational concentration groups ((N = 2) per group, total (N = 10)) were determined using a standard one-way Analysis of Variance (ANOVA). Trends and predictive relationships for Chemical Oxygen Demand (COD) removal efficiency and dye decolorization efficiency as a function of the operational parameter (dye concentration) were evaluated using simple linear regression models. For all statistical tests, we set the significance threshold a priori at $\alpha = 0.05$. Because these are repeated measurements from the same reactors, we treated them as temporal rather than independent biological replicates. The regressions were fitted to the final (cycle 22) values of the five concentrations ($n = 5$).

3. Results and Discussion

3.1. Decolorization Performance of Microbial Fuel Cells

The MO dye decolorization in the aqueous-cathode dual-chamber MFCs at an external resistance of 100 ohm was investigated at different concentrations in the range of 20–100 mg/L using synthetic wastewater with acetate as a co-substrate. The decolorization efficiency of the MFC reactors was calculated using Equation (3). As shown in Figure 2, all MFCs decolorized the dye. In the initial stage (the first five cycles), removal efficiency remained below 50% in all reactors, indicating that the microbial community needed time to acclimatize to the dye-containing environment. As operation progressed, decolorization efficiency steadily increased, reaching 83–90% by cycle 20 and remaining stable until cycle 22 within 3–4 h. Steady-state variation was less than 5% in all MFCs, demonstrating consistent reactor performance.

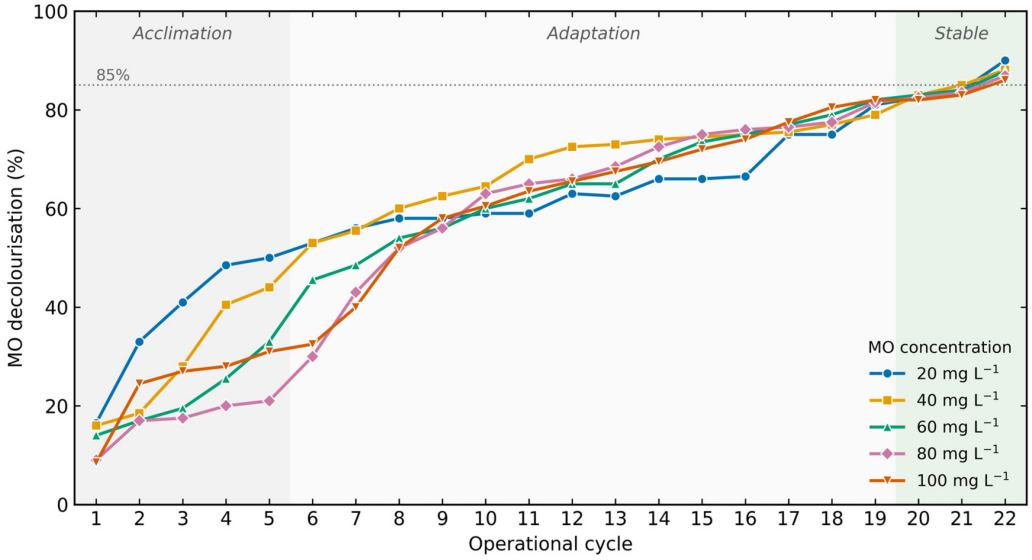


Figure 2. Methyl orange (MO) decolorization (%) in MFCs operated at 20–100 mg L^{-1} over 22 operational cycles. Shaded regions indicate the acclimation, adaptation, and stable phases.

The effect of dye concentration was evident during the early cycles (Figures 2 and S1). As MO dye concentration increased from 20 to 100 mg L^{-1}, initial decolorization efficiency remained low (10–30%) for the first six cycles. Compared with the high dye concentration (60–100 mg/L), the lower MO dye concentrations (20–40 mg/L) achieved a faster decolorization rate, reaching 50% within 5 cycles. However, after microbial acclimation, all MFCs achieved stable decolorization efficiencies above 85%, indicating that the anodic microbial community effectively adapted to elevated dye concentrations. Similar improvements have been reported in MFC systems treating MO, where acclimated microbial consortia showed enhanced extracellular electron transfer and sustained dye removal under prolonged operation [13,14]. The decrease in residual dye concentration further confirmed the treatment efficiency. At the end of the cycle, in MFC-1 (20 mg/L), the absorbance at 465 nm decreased from 1.2 to 0.12 by the 22nd cycle. Similarly, MFC-2, MFC-3, MFC-4, and MFC-5 showed reductions from 1.6 to 0.19, 1.8 to 0.22, 2.3 to 0.30, and 2.5 to 0.35, respectively. Overall, dye removal in all reactors remained above 85%, although reactors treating higher dye concentrations showed slightly higher residual absorbance. This points towards stable treatment performance even under varying dye loadings. The decrease in the characteristic MO absorbance peaks during treatment is shown in Figure S4.

At higher concentrations, the gradual improvement in decolorization suggests adaptation and enrichment of electroactive microorganisms capable of reducing azo dyes. Joksi-

mović et al. [19] reported similar observations while investigating Reactive Black 5 (dye) decolorization. Their study achieved nearly 98% decolorization at an initial dye concentration of 25 mg L^{-1} within 2 h, but increasing the dye concentration to 50 mg/L prolonged the treatment time and required a higher H_2O_2 dosage to achieve comparable removal. These findings show that higher dye loading slows decolorization kinetics and increases the demand for reducing equivalents during azo dye transformation. In the present study, we observed a similar concentration-dependent response during the initial operational cycles; however, prolonged operation enabled microbial acclimation, resulting in stable decolorization efficiencies across all concentrations. In MFCs, microorganisms oxidize available substrates in the anolyte and release electrons. The released electrons are transferred to the anode, or, alternatively, to azo dyes, which act as electron acceptors and undergo reductive transformation. The primary mechanism involves cleavage of the azo bond (-N=N-), which leads to the breakdown of the dye structure and loss of color [20]. In the present study, spectral analysis supported these observations. The reduction was more noticeable in reactors operated at lower dye concentrations, particularly MFC-1. The dye concentration in the samples remained after treatment and was also determined within the 5-h time range using Beer–Lambert's law (Figure S1). Methyl Orange (an azo dye, R − N = N − R′) and its byproducts can serve as additional carbon sources or undergo mediated electron transfer, supporting exoelectrogenic biofilm growth and enhancing chemical oxygen demand (COD) removal. Although MO acts as an electron acceptor and generates current at low to optimal concentrations, dye decolorization of methyl orange also occurs via azo bond cleavage [14]. Adsorption of MO onto the carbon felt, the clayware, and the biomass, as well as other non-bioelectrochemical processes, may also contribute to color removal. Two observations indicate that adsorption was not the dominant mechanism during long-term operation. First, fresh MO-containing anolyte was supplied to the same electrodes in every cycle for 22 cycles, so removal by adsorption alone would be expected to decline as sorption sites became saturated, whereas decolorization increased progressively from below 50% to 86–90% (Figure 2). Second, this increase followed the same time course as the rise in cell voltage and current (Figure 3A,B), consistent with the development of an active anodic biofilm. However, abiotic and open-circuit control data are not reported in the present study, so the relative contributions of adsorption, biological reduction, and bioelectrochemical reduction could not be quantified.

The results show that MFCs can efficiently and stably decolorize MO dye over a wide concentration range. Although higher dye concentrations initially suppressed performance, the system adapted with continued operation, resulting in high removal efficiencies and low residual dye concentrations at steady state.

3.2. Phytotoxicity Test

The phytotoxicity of treated and untreated MO-containing wastewater was evaluated using *Pisum sativum* seeds by monitoring seed germination rate, root elongation, and shoot growth. Clear differences were observed between untreated dye samples and MFC-treated effluents across all concentrations (20–100 mg/L). Seeds exposed to untreated dye solutions showed severely inhibited growth, with only minimal root elongation on day 1 (1–4 mm) and no further development, indicating strong influent toxicity. In contrast, effluents obtained after MFC treatment supported seed germination and subsequent growth. By day 5, root lengths reached approximately 20–22.5 mm and shoot lengths 25–27 mm across all treated samples, demonstrating substantial recovery of plant growth (Figure S2).

Among the tested conditions, higher concentrations (80–100 mg/L) showed marginally reduced elongation compared with lower dye concentrations (20–40 mg/L), although they remained markedly better than the untreated samples. The control (distilled water) showed

the highest growth, with root and shoot lengths reaching 32 mm and 40 mm, respectively, confirming the absence of inhibitory effects.

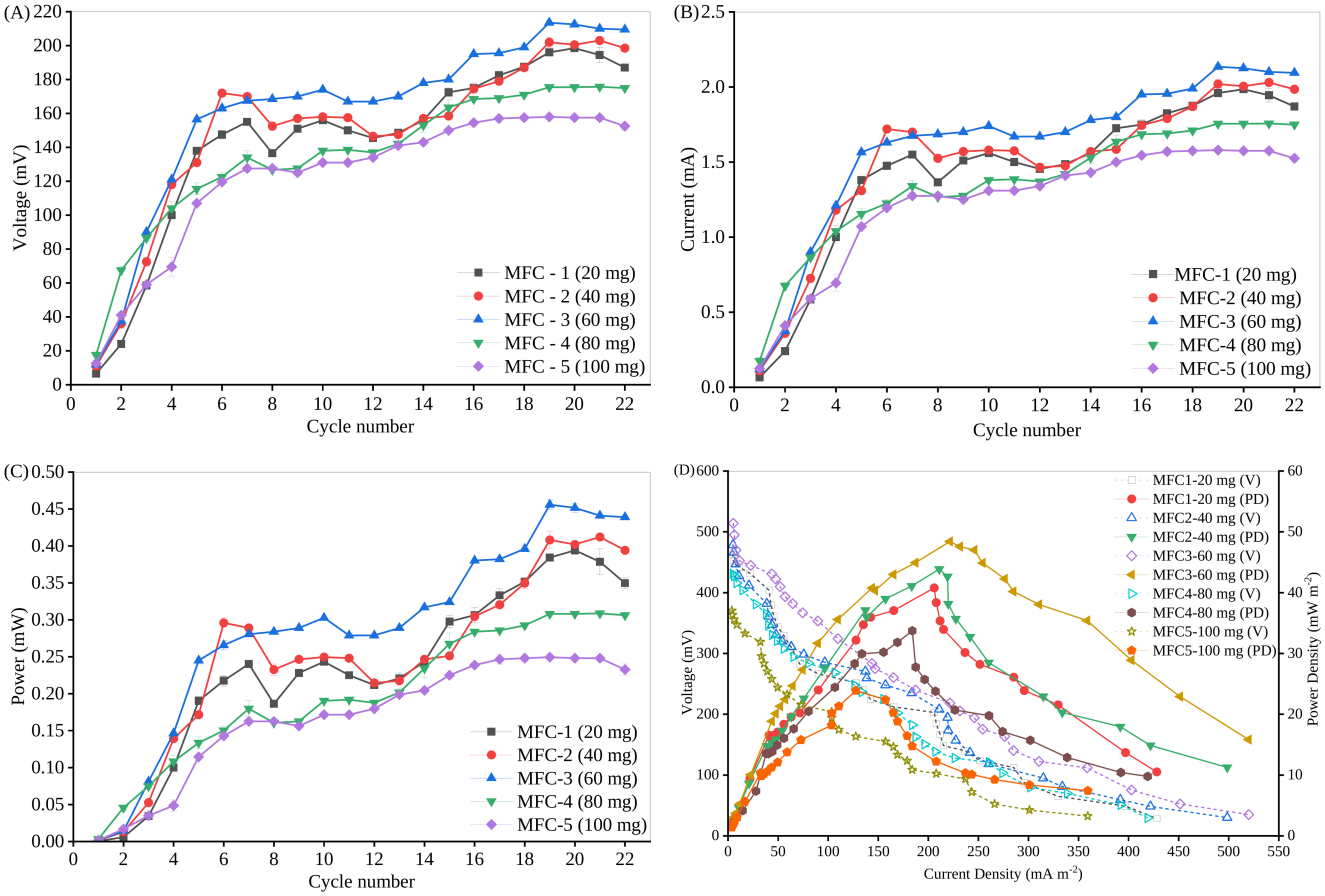


Figure 3. Performance of MFC reactors at varying methyl orange dye concentrations in the anode chamber: (**A**) voltage generation, (**B**) current generation, (**C**) power output, and (**D**) polarization curves.

Growth inhibition analysis further supported these observations. Initial inhibition rates were high (50–57%) on day 1 across all concentrations, but decreased progressively over time, reaching 32–37% by day 5. This trend indicates gradual detoxification of the effluent during MFC treatment. The results show that MFC treatment effectively reduces the phytotoxicity of MO dye-containing wastewater, improving seed germination and plant growth. This reduction in toxicity can be attributed to byproducts and the microbial transformation of dye compounds into less harmful intermediates. The seed germination rate of the respective samples was also noted (Figure S3). The control sample (distilled water) attained 100% seed germination. As dye concentration increased, the germination rate decreased in seeds incubated with the initial dye wastewater, whereas MFC-treated samples achieved a maximum germination rate comparable to the control. At the end of incubation, the seeds achieved germination rates of 100% for MFC-20 mg, 100% for MFC-40 mg, 90% for MFC-60 mg, 90% for MFC-80 mg, and 80% for MFC-100 mg, respectively. The results indicate that treatment reduced toxicity.

3.3. Voltage, Current and Power Generation in Microbial Fuel Cells

All MFCs were initially operated in open-circuit conditions for a week to promote microbial colonization on the anode, until a constant open-circuit voltage (OCV) of 500 ± 5 mV was attained. Later, the reactors were operated under closed-circuit conditions by connect-

ing the electrodes with an external resistor (100 Ω). The MFCs achieved stable performance after approximately 22 operational cycles (88 days). During the initial phase (cycles 1–5), voltage generation remained low (<100 mV) (Figure 3A), likely because the mixed microbial culture was acclimating to dye-containing wastewater. Correspondingly, the current output was also limited (1.0–1.5 mA) (Figure 3B), indicating slow establishment of electroactive biofilms. Nevertheless, operation continued because decolorization efficiency remained low (<50%). From cycle 6 onward, performance improved clearly. The voltage output gradually increased and stabilized at 140–220 mV by cycle 22, while current generation improved to approximately 1.5–2.2 mA. This trend indicates that current generation increased because the microorganisms effectively transferred electrons to the anode through acetate oxidation.

Among the reactors, MFC-3 (60 mg/L) generated the highest voltage, reaching a maximum of 210–215 mV (cycles 19–22). MFC-2 (40 mg L^{-1}) followed at 205 mV, and MFC-1 (20 mg L^{-1}) at 197 mV. In contrast, MFC-4 (80 mg L^{-1}) and MFC-5 (100 mg L^{-1}) showed comparatively lower voltages of 176 mV and 159 mV, respectively. The voltage reduction at MO concentrations above 60 mg L^{-1} suggests that higher pollutant levels inhibited electrogenic microorganisms and diverted electrons toward MO reduction, reducing electron flow to the anode. For comparison, Joksimović et al. [19] obtained an average voltage of 295 mV during the decolorization of 25 mg L^{-1} Reactive Black 5 (RB5). The comparatively lower voltages observed in the present study can be attributed to higher dye concentrations (20–100 mg L^{-1}), which likely stressed the microbial community more and reduced its electrochemical activity.

Once the reactors reached stable voltages, we performed a polarization test to investigate their potential power density. To maintain stable power output, operate a reactor at an external resistance similar to the internal resistance obtained from the polarization experiment. MFC-3 achieved the highest power density (48 mW m^{-2}), followed by MFC-2 (44 mW m^{-2}) and MFC-1 (41 mW m^{-2}) (Figure 3D). In comparison, MFC-4 (34 mW m^{-2}) and MFC-5 (23 mW m^{-2}) recorded lower power densities (Table 1). MFC-3's superior performance indicates that a moderate dye concentration (60 mg L^{-1}) balances substrate availability and microbial tolerance. These values are the maximum power densities obtained from the polarization curves. During routine operation at a fixed external resistance of 100 Ω, the power densities calculated from the maximum stable cell voltages (P = V2/Rext) were 39.2, 42.4, 46.7, 31.3, and 25.5 mW m^{-2} for MFC-1 to MFC-5, respectively (Figure 3C). The 100 Ω load was close to the internal resistance of MFC-3 (90 Ω), but about half that of MFC-5 (200 Ω), so MFC-5 operated further from its maximum power point. The slightly higher operating value than the polarization maximum for MFC-5 arises because polarization was performed once, at the end of operation, whereas the operating value corresponds to the highest voltage recorded during cycles 19–22.

Table 1. Comparative representation of methyl orange dye decolorization and energy production in different MFC reactors.

Reactor	Dye Concentration (mg L^{-1})	Maximum Voltage (mV)	Maximum Power Density (mW m^{-2})	Maximum Current Density (mA m^{-2})	Maximum Dye Decolorization (%)	COD Removal Efficiency (%)
MFC-1	20	197	41	428	90.0	70.6
MFC-2	40	205	44	498	88.1	71.9
MFC-3	60	215	48	520	87.8	72.2
MFC-4	80	176	34	419	86.9	73.3
MFC-5	100	159	23	359	86.0	73.8

The power densities obtained in the present study were higher than those reported for several other dye-degrading fuel-cell systems. Khalik et al. [21] reported power den-

sities of 1.67–15.19 mW m^{-2} during the treatment of Reactive Black 5 (RB5) at concentrations of 20–50 mg L^{-1}. Similarly, Joksimović et al. [19] reported a power density of only 3.42 mW m^{-2} during the degradation of 25 mg L^{-1} RB5 in the presence of H_2O_2, although they achieved approximately 98% dye decolorization. In contrast, the present study achieved power densities of 23–48 mW m^{-2} while treating higher MO concentrations (up to 100 mg L^{-1}), indicating good electrochemical performance even under increased dye loading. However, the maximum power density was lower than the 134 mW m^{-2} reported by Chacko et al. [16] with the same heat-pretreated inoculum but at a much lower MO concentration (25 mg L^{-1}) and over a shorter operating period, indicating that the higher dye loadings used here reduced the electron flow to the anode. These results indicate that the developed MFC system can achieve stable electricity generation and effective dye decolorization with heat-pretreated inoculum, even at higher MO concentrations.

To evaluate the effect of MO concentration on the bioelectrochemical behavior and charge-transfer kinetics of the MFCs, CV and LSV analyses were conducted for all reactors. In CV, the maximum oxidation currents were 0.25, 0.20, 0.18, 0.15, and 0.11 A for MFC-5, MFC-4, MFC-3, MFC-2, and MFC-1, respectively (Figure 4A), indicating that the voltammetric current increased with MO concentration. These voltammetric currents (0.11–0.25 A) are not directly comparable with the operating currents (1.5–2.2 mA). They are transient currents recorded while the potential was swept over a wide window (−1 to +1 V vs. Ag/AgCl) on a high-surface-area carbon felt electrode and therefore include capacitive charging of the electrode–biofilm interface and faradaic contributions from MO, its reduction intermediates and, at the potential extremes, water reduction and oxidation. By contrast, the operating current is the steady-state current through the 100 Ω loads. The oxidation and reduction peaks across the potential range indicate microbially mediated catalytic reactions [22]. However, this trend is opposite to that of cell voltage, power density, and CE, which were lowest at 100 mg L^{-1}. The higher voltammetric current at elevated MO concentrations is therefore mainly attributed to the redox activity of MO and its reduction intermediates adsorbed on or near the electrode, along with capacitive charging, rather than enhanced electrogenic activity. During the CV scan, the imposed potential drives the oxidation and reduction of these redox-active species near the anode, producing a larger current envelope. At the same time, dye accumulation and toxic by-products on the electrode surface can passivate catalytic sites and stress the anodic microbial community, consistent with the higher internal resistance and lower steady-state power observed at 100 mg L^{-1}.

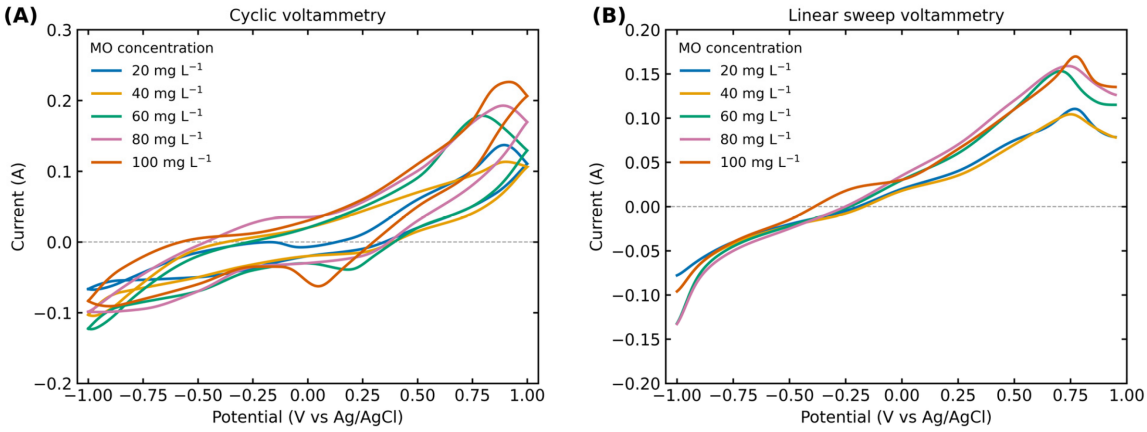


Figure 4. Performance of MFCs with different dye concentrations based on electrochemical activity: (**A**) cyclic voltammetry and (**B**) linear sweep voltammetry.

We conducted linear sweep voltammetry (LSV) across all five MFC configurations (20–100 mg/L MO) to evaluate how Methyl Orange (MO) concentration affects anodic

bioelectrocatalysis and charge-transfer kinetics (Figure 4B). MFC5-100 mg achieves the highest peak current at approximately 0.18 A at around 0.75 V, followed by MFC4-80 mg. In contrast, MFC1-20 mg and MFC2-40 mg display the lowest current responses. Consistent with the CV results, this higher current reflects the contribution of redox-active MO species rather than improved bioelectrocatalysis, since the steady-state power output followed the opposite trend. Because voltammetry is a dynamic technique in which the potential is swept rapidly, it also captures transient capacitive charging of the biofilm and redox-active intermediates and therefore differs fundamentally from steady-state polarization [23].

The internal resistance, derived from the polarization graph, was considerably higher in MFC-5 (200 Ω), whereas MFC-3 showed a notably lower internal resistance of 90 Ω. This lower internal resistance in MFC-3 may be attributed to enhanced electrogenic activity driven by improved biofilm development on the anode surface, as Chacko et al. [16] previously reported. Moreover, reduced ohmic and mass-transport losses in MFC-3 may reflect improved substrate utilization by the electrogenic consortium, driven by optimal dye concentration and microbial activity.

In the present study, the reduced power output at higher dye concentrations may reflect increased internal resistance and mass-transfer limitations, which negatively affect electron transport. Additionally, higher dye concentrations may interfere with biofilm development and electron-transfer pathways, reducing electrochemical efficiency. Therefore, the results show that while MFCs can simultaneously decolorize dye and generate electricity, increasing dye concentration adversely affects power production. Among the tested concentrations, 60 mg L^{-1} was optimal for achieving maximum electrochemical performance without severe inhibitory effects. Because decolorization remained above 85% up to 100 mg L^{-1}, the treatable range extends to at least 100 mg L^{-1}; however, increasing the concentration from 60 to 100 mg L^{-1} reduced power density by approximately 52% and coulombic efficiency by approximately 30%. Where energy recovery is a priority, influents exceeding 60–80 mg L^{-1} MO would therefore benefit from dilution or staged treatment.

3.4. Efficiency of Microbial Fuel Cell: COD Removal and Coulombic Efficiency

The performance of the MFC reactors was evaluated for their COD removal efficiency (Equation (1)) and coulombic efficiency (CE) (Equation (2)). Figure 5A illustrates the variation in COD removal efficiency at different MO dye concentrations during long-term operation, with each reactor operated for 22 cycles over 88 days. Initially, all the reactors exhibited comparatively lower COD removal efficiencies, indicating the acclimation phase of the anodic microbial community. By cycle 4, COD removal efficiencies ranged from 41–42% in MFC-1 (20 mg L^{-1}) to 54–55% in MFC-5 (100 mg L^{-1}).

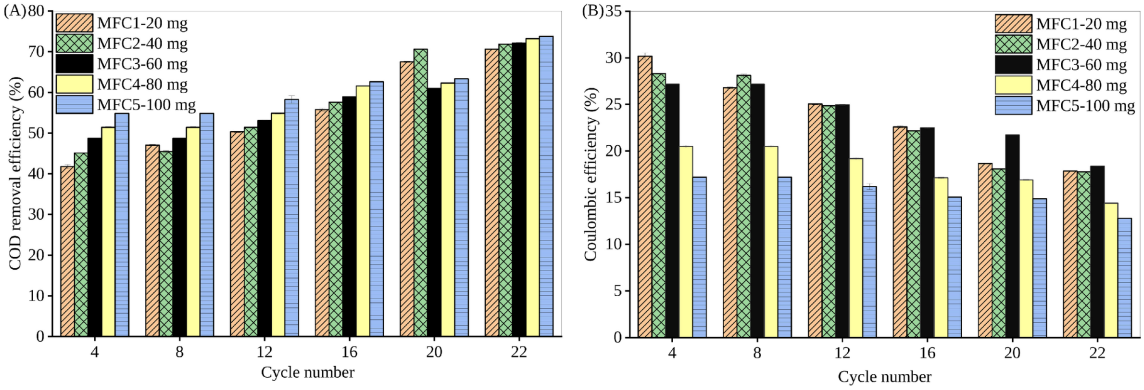


Figure 5. Effect of methyl orange dye concentration on (**A**) COD removal efficiency and (**B**) coulombic efficiency of MFCs during 22 operational cycles.

As the operational cycles progressed, all reactors showed a gradual increase in COD removal efficiency, suggesting effective adaptation and enrichment of electroactive microorganisms. By cycle 12, COD removal efficiencies increased to approximately 50–59%, while after cycle 16 the reactors consistently achieved values above 55%. After cycle 20, reactor performance stabilized, with COD removal efficiencies reaching approximately 70–74% across all reactors.

At the end of the 22nd cycle, the maximum COD removal efficiencies achieved were 70.6%, 71.9%, 72.2%, 73.3%, and 73.8% for MFC-1 to MFC-5, respectively. Correspondingly, COD concentrations decreased from 3030, 3065, 3100, 3180, and 3210 mg L^{-1} to 890, 860, 862, 849, and 841 mg L^{-1} in MFC-1 to MFC-5, respectively, confirming efficient organic matter degradation during prolonged operation.

The gradual improvement in COD removal indicates that the anodic microbial consortium adapted to increasing dye concentrations without significantly inhibiting microbial metabolism. The slightly higher COD removal efficiencies at elevated dye concentrations may reflect enhanced microbial utilization of organic intermediates generated during azo dye reduction. In MFC systems, electroactive microorganisms oxidize acetate at the anode, releasing electrons and protons, while the azo dye acts as an electron acceptor during reductive decolorization. The stable reactor performance throughout the study demonstrates that the developed earthen-membrane cylindrical MFC maintained effective substrate utilization and electrogenic activity even under higher dye-loading conditions. As dye concentration exceeds the optimal threshold, azo dye toxicity and reductive-cleavage metabolites (such as aromatic amines like sulfanilic acid and *N*,*N*-dimethyl-*p*-phenylenediamine) stress the anodic microbial community. This inhibits exoelectrogenic activity, reducing both Coulombic efficiency and overall COD removal [24]. MO can act as an alternative electron acceptor because of the azo bond (–N=N–). As a result, two main pathways compete for electrons released during the oxidation of organic matter: (1) Electrical current is produced when electrons are moved from exoelectrogens to the anode surface by direct contact or mediators (such as cytochromes or synthetic or natural mediators). (2) The azo bonds of MO are directly reduced by electron interception in the bulk solution or by non-exoelectrogenic suspended biomass. Pathway 2 predominates over anodic transfer at greater dye concentrations, serving as an internal "electron sink." This explains why, even when apparent COD removal appears sustained through adsorption or incomplete mineralization, higher initial dye loadings can decrease power density and Coulombic efficiency [22].

The CE (%) of the MFC reactors was also evaluated to determine the fraction of electrons recovered as electrical current relative to the total electrons available in the substrate. CE values were higher during the initial operational cycles, then gradually declined with increasing cycle number (Figure 5B). By cycle 4, MFC-1 (20 mg L^{-1}) had the highest CE at approximately 30%, whereas MFC-4 (80 mg L^{-1}) and MFC-5 (100 mg L^{-1}) showed lower values of around 20% and 17%, respectively. Similar trends were observed throughout the operational period, and by the 22nd cycle the CE decreased to 17.8%, 17.8%, 18.4%, 14.4%, and 12.8% for MFC-1 to MFC-5, respectively. The decline in CE over time, despite increased current output, reflects faster COD removal, indicating that a growing fraction of the substrate was consumed through non-electrogenic pathways such as fermentation and methanogenesis, which heat pretreatment of the inoculum may suppress only temporarily during long-term operation.

The comparatively higher CE observed in MFC-1 and MFC-2 indicates more efficient electron recovery from acetate oxidation by electroactive microorganisms under lower dye concentrations. In contrast, the reduction in CE at elevated dye concentrations suggests that a larger fraction of electrons was diverted toward azo dye reduction and other competing metabolic pathways rather than electricity generation. Higher dye loading may also inhibit

exoelectrogenic activity, reducing electron transfer efficiency to the anode. Despite the decline in CE at higher dye concentrations, all reactors maintained stable decolorization and COD removal efficiencies, demonstrating the anodic microbial consortium's ability to sustain simultaneous wastewater treatment and bioelectricity generation during prolonged operation.

Chacko et al. [16] reported similar findings, operating earthen membrane cylindrical MFCs fed with 3 g L^{-1} acetate and 25 mg L^{-1} methyl orange using heat-treated and untreated mixed anaerobic cultures. The heat-pretreated reactor showed higher coulombic efficiency (25%) than the untreated system (13.7%), attributed to suppressed methanogens and enriched exoelectrogenic bacteria. In the present study, which also used heat-pretreated inoculum, CE values of 17.8–18.4% were maintained at 20–60 mg L^{-1} after 22 cycles, lower than the 25% reported at 25 mg L^{-1} [16], indicating stable electrogenic activity and efficient substrate utilization during long-term operation. However, increasing dye concentration gradually reduced CE, likely because more electron consumption occurs during azo dye reduction and other competing microbial pathways.

3.5. Performance Comparison with Existing Studies

The performance of the present study was compared with previously reported MFC systems for dye decolorization and simultaneous electricity generation (Table 2). Earlier studies showed that dye removal efficiency and power generation depend strongly on reactor configuration, inoculum type, operating conditions, and dye concentration. Chacko et al. [16] achieved complete methyl orange decolorization within 4 h and produced a maximum power density of 134 mW m^{-2}, whereas the untreated reactor generated only 24.5 mW m^{-2} with 80% decolorization. The improved performance was attributed to methanogen suppression, enrichment of electroactive microorganisms, and enhanced electron recovery. In the present study, the maximum power density was 48 mW m^{-2} at 60 mg L^{-1} methyl orange. Although this value was lower than that of the heat-pretreated system, the present reactors were operated at up to four times higher MO concentrations (up to 100 mg L^{-1}) and over a longer operating period. More importantly, the present study maintained stable decolorization efficiencies of 86–90% over 22 operational cycles, demonstrating stable long-term electrogenic activity under higher dye concentrations (20–100 mg L^{-1}).

The electrical performance in the present study was comparable to previously reported dye-degrading fuel-cell systems. For example, Joksimović et al. [19] reported an average voltage of 295 mV and a power density of only 3.42 mW m^{-2} during the degradation of 25 mg L^{-1} Reactive Black 5 using an MFC-assisted electro-Fenton system, while Khalik et al. [21] reported power densities ranging from 1.67 to 15.19 mW m^{-2} for Reactive Black 5 concentrations of 20–50 mg L^{-1}. The higher power densities achieved in the present study (23–48 mW m^{-2}) indicate efficient electricity generation despite operating at higher methyl orange concentrations.

Furthermore, Agrahari et al. [11] achieved power densities of 225–474 mW m^{-2} with >84% dye decolorization using *Pseudomonas gessardii* in H-type dual-chamber MFCs. Similarly, Mittal et al. [20] reported 94.2% methyl orange decolorization at 148 mW m^{-2} in an earthen membrane constructed wetland-MFC system operated for 270 days, while Khan et al. [25] achieved 94% Acid Blue 29 removal at 77.3 mW m^{-2} in a single-chamber MFC. Shahi et al. [26] also demonstrated nearly complete reactive orange decolorization using mixed bacterial consortia, though with moderate power generation (84 mW m^{-2}), while Mani et al. [22] observed only 20% Acid Orange 7 decolorization with *Shewanella oneidensis*, indicating that reactor configuration and microbial adaptability strongly influence dye degradation performance. The study has limitations: it did not study ion transport across

the membrane or the effects of the anolyte and catholyte on ceramic composition during the experiment.

Table 2. Comparison of MFC performance in terms of dye decolorization and electricity generation with previous MFC studies.

MFC Type	Volume (mL)	Inoculum	Dye	Power Density (mW m^{-2})	Maximum Dye Decolourisation (%)	References
Earthen membrane-Cylindrical MFC	150	*Anaerobic mixed culture-heat treated*	Methyl Orange-20 mg L^{-1}	41	90.0	This study
Earthen membrane-Cylindrical MFC	150	*Anaerobic mixed culture-heat treated*	Methyl Orange-40 mg L^{-1}	44	88.1	This study
Earthen membrane-Cylindrical MFC	150	*Anaerobic mixed culture-heat treated*	Methyl Orange-60 mg L^{-1}	48	87.8	This study
Earthen membrane-Cylindrical MFC	150	*Anaerobic mixed culture-heat treated*	Methyl Orange-80 mg L^{-1}	34	86.9	This study
Earthen membrane-Cylindrical MFC	150	*Anaerobic mixed culture-heat treated*	Methyl Orange-100 mg L^{-1}	23	86.0	This study
Earthen membrane-Cylindrical MFC	300	*Anaerobic mixed culture*	Methyl Orange-25 mg L^{-1}	24.5	80	[16]
Earthen membrane-Cylindrical MFC	300	*Anaerobic mixed culture-heat treated*	Methyl Orange-25 mg	134	100	[16]
H-type MFC	300	*Pseudomonas gessardii*	Reactive Black 5	474	98.5 ± 2.1	[11]
H-type MFC	300	*Pseudomonas gessardii*	Reactive Red 120	262	95 ± 2.9	[11]
H-type MFC	300	*Pseudomonas gessardii*	Coomassie Brilliant Blue	225	84.5 ± 3.4	[11]
Earthen membrane CW-MFC	250	Mixed-culture	Methyl Orange	148	94.22 ± 1.33	[20]
SMFC	300	Mixed-culture activated sludge	Acid Blue 29	77.3 ± 3.4	94 ± 1.9	[25]
DCMFC	450	Mixed bacterial consortium	Reactive Orange	84	Around 100	[26]
H-type MFC	200	*S. oneidensis*	Acid Orange 7	42.5 ± 2.6	20	[22]

In summary, this study demonstrated efficient, stable methyl orange decolorization across varying dye concentrations using a low-cost earthen membrane-cylindrical MFC operated over prolonged cycles. While the power densities were comparatively lower than those reported for optimized pure-culture or heat-treated systems, the sustained long-term operation and consistent decolorization efficiency highlight the practical applicability of the developed MFC system for long-term dye-containing wastewater treatment.

3.6. Statistical Evaluation of Data

3.6.1. Electrochemical Performance (Power Density & Coulombic Efficiency)

The initial dye concentration significantly influenced the system's electrochemical performance. A mathematically rigorous One-way ANOVA confirmed that the variations in Coulombic efficiency across the distinct operational groups were highly statistically significant ($(F(4, 5) = 3465.44)$, $(p < 0.001)$). Similarly, variations in sustainable power density among the configurations showed strong statistical significance ($(F(4, 5) = 628.27)$, $(p < 0.001)$). These findings show that changes in the initial substrate or pollutant loading directly alter the anodic biofilm's internal resistance and metabolic pathways, leading to distinct, highly reproducible electrical output profiles. These analyses used CE values from six COD sampling events in each of the two duplicate reactors ($n = 12$ per concentration) and cycle-wise power densities over 22 cycles ($n = 22$ per concentration). Because these are

repeated measurements from the same reactors, the results show that differences between concentrations were consistent throughout operation; they should not be interpreted as independent biological replicates, of which there were two per concentration.

3.6.2. Wastewater Treatment Profile (COD Removal Efficiency)

Organic matter degradation depended strongly on operational loading. Linear regression analysis revealed a statistically significant positive relationship between the initial dye concentration (X) and COD removal efficiency ($t = 9.57$, $p = 0.0024$). The predictive linear model was established as (COD Removal (%) = 70.03 + 0.038X), yielding a slope coefficient of 0.038 (95% CI: 0.025 to 0.051). This positive correlation suggests that, within the evaluated range, a higher initial concentration provides a larger substrate gradient, accelerating microbial metabolic activity and organic removal rates.

3.6.3. Decolorization Kinetic Profile (Dye Decolorization Efficiency)

In contrast to organic removal trends, the dye decolorization efficiency exhibited an inverse relationship with increasing concentration. Simple linear regression demonstrated a statistically significant negative trend ($t = -7.07$, $p = 0.0058$), following the predictive model equation: (Dye Decolorization (%) = 90.52 − 0.046X). The negative slope coefficient (−0.046) (95% CI: −0.067 to −0.025) indicates that increasing the initial dye concentration predictably reduces decolorization efficiency. Although statistically significant, this decline was modest (approximately 4 percentage points across the tested range) and likely reflects saturation of azo-reducing enzymes and active degradation sites, or minor toxicity effects at elevated dye loading.

4. Conclusions

The present study demonstrated the applicability of earthen membrane cylindrical microbial fuel cells for simultaneous methyl orange decolorization and bioelectricity generation under varying dye concentrations. The reactor maintained stable performance over 22 operational cycles, with decolorization efficiencies above 85% across all tested concentrations (20–100 mg L^{-1}). The highest power density (48 mW m^{-2}) occurred at 60 mg L^{-1}, while higher dye concentrations reduced electrochemical performance, indicating inhibitory effects. Considering decolorization, power output, and coulombic efficiency together, 60 mg L^{-1} is the optimal MO concentration for this system, while concentrations up to 100 mg L^{-1} can still be treated effectively (>85% decolorization) when energy recovery is a secondary objective. Collectively, the findings highlight the potential of earthen membrane MFCs as sustainable bioelectrochemical systems for treating dye-containing wastewater while simultaneously recovering bioenergy. Further optimization of electrode materials, reactor hydrodynamics, and microbial enrichment strategies may improve power generation and support scale-up for practical wastewater treatment applications. While this study demonstrates the system's promising efficacy, several methodological constraints should be considered when interpreting the results. The system's resilience under prolonged operation remains untested, and the anodic microbial community and biofilm are not characterized, so the proposed enrichment of electroactive microorganisms remains unconfirmed. In addition, the authors did not report abiotic and open-circuit controls, so they did not quantify the contributions of adsorption and non-bioelectrochemical reduction to decolorization. Future work addressing these long-term operational, matrix-complexity, and multi-omic challenges will be critical to validating and scaling this technology for full-scale applications.

Supplementary Materials: The following supporting information can be downloaded at https://www.mdpi.com/article/10.3390/en19215136/s1, Figure S1: Heat map of methyl orange (MO) decolorization (%) by dye concentration (20–100 mg L^{-1}) and operational cycle. White lines separate the acclimation (cycles 1–5), adaptation (cycles 6–19) and stable (cycles 20–22) phases. Values correspond to those shown in Figure 2 of the main text; Figure S2: UV–Vis spectra (200–700 nm) recorded before and after MFC treatment for a single dye concentration; Figure S3: Residual MO, determined from absorbance at 465 nm using the Beer–Lambert law, during the first 5 h of a cycle and at the end of the cycle (96 h) for initial MO concentrations of 20–100 mg L^{-1}; Figure S4: Phytotoxicity of MO-containing anolyte towards Pisum sativum seeds. (A) Seed germination after incubation with anolyte collected before (BT) and after (AT) MFC treatment at each MO concentration, and with distilled water (control). (B) Seed germination rate (%) for the control, BT and AT samples.

Author Contributions: Conceptualization, P.P.R., P.C. and M.T.N.; methodology, A.C., N.K.C. and P.P.R.; validation, N.K.C. and M.T.N.; formal analysis, writing—review and editing, N.K.C.; investigation, N.K.C.; resources, P.P.R.; data curation, A.C. and N.K.C.; writing—original draft preparation, N.K.C. and V.S.; writing—review and editing, A.C., N.K.C., V.S., P.C., M.T.N. and P.P.R.; visualization, A.C., N.K.C. and P.P.R.; supervision, P.C. and P.P.R.; project administration, P.C. and P.P.R.; funding acquisition, P.P.R.; formal analysis, S.P.S. All authors have read and agreed to the published version of the manuscript.

Funding: The grant received from University Grant Commission, Govt. of INDIA [File No. F.30-566/2021(BSR)], to undertake this work is duly acknowledged. Md Tabish Noori received support from the Ramon y Cajal project grant (RYC2024-049008-I). Narnepati Krishna Chaitanya and Pritha Chatterjee would like to thank the Department of Civil Engineering (IIT Hyderabad) for their financial support and laboratory provided for this project.

Institutional Review Board Statement: Not applicable.

Informed Consent Statement: Not applicable.

Data Availability Statement: The data presented in this study are available on request from the corresponding authors.

Acknowledgments: N.K.C. and P.C. thank the Department of Civil Engineering, Indian Institute of Technology Hyderabad, for financial support and laboratory facilities provided for this project.

Conflicts of Interest: The authors declare no conflicts of interest.

References

1. Rahimnejad, M.; Adhami, A.; Darvari, S.; Zirepour, A.; Oh, S.E. Microbial fuel cell as new technology for bioelectricity generation: A review. *Alex. Eng. J.* **2015**, *54*, 745–756. [CrossRef]
2. Shajid, S.R.; Mourshed, M.; Kibria, M.G.; Shabani, B. The Potential of Microbial Fuel Cells as a Dual Solution for Sustainable Wastewater Treatment and Energy Generation: A Case Study. *Energies* **2025**, *18*, 3725. [CrossRef]
3. Mandal, S.K.; Das, N. Application of microbial fuel cells for bioremediation of environmental pollutants: An overview. *J. Microbiol. Biotechnol. Food Sci.* **2018**, *7*, 437–444. [CrossRef]
4. Islam, S.; Jalil, M.A.; Hossain, S.; Belowar, S.; Saeed, M.A. Balancing performance and sustainability: A comparative analysis of natural and synthetic dyes. *Heliyon* **2026**, *12*, e45100. [CrossRef]
5. Oon, Y.S.; Ong, S.A.; Ho, L.N.; Wong, Y.S.; Oon, Y.L.; Lehl, H.K.; Thung, W.E.; Nordin, N. Disclosing the synergistic mechanisms of azo dye degradation and bioelectricity generation in a microbial fuel cell. *Chem. Eng. J.* **2018**, *344*, 236–245. [CrossRef]
6. Rawat, D.; Sharma, R.S.; Karmakar, S.; Arora, L.S.; Mishra, V. Ecotoxic potential of a presumably non-toxic azo dye. *Ecotoxicol. Environ. Saf.* **2018**, *148*, 528–537. [CrossRef] [PubMed]
7. Zafar, S.; Bukhari, D.A.; Rehman, A. Azo dyes degradation by microorganisms—An efficient and sustainable approach. *Saudi J. Biol. Sci.* **2022**, *29*, 103437. [CrossRef] [PubMed]
8. Haque, M.M.; Haque, M.A.; Mosharaf, M.K.; Marcus, P.K. Decolorization, degradation and detoxification of carcinogenic sulfonated azo dye methyl orange by newly developed biofilm consortia. *Saudi J. Biol. Sci.* **2021**, *28*, 793–804. [CrossRef] [PubMed]
9. Tripathi, A.; Srivastava, S.K. Ecofriendly treatment of azo dyes: Biodecolorization using bacterial strains. *Int. J. Biosci. Biochem. Bioinform.* **2011**, *1*, 37. [CrossRef]

10. Wang, H.; Wang, Q.; Li, X.; Wang, Y.; Jin, P.; Zheng, Y.; Huang, J.; Li, Q. Bioelectricity generation from the decolorization of reactive blue 19 by using microbial fuel cell. *J. Environ. Manag.* **2019**, *248*, 109310. [CrossRef] [PubMed]
11. Agrahari, R.; Karmakar, S.; Rani, R. Bioelectricity generation and anodic decolorization of reactive dyes in H-type microbial fuel cell using *Pseudomonas gessardii*. *Environ. Chem. Ecotoxicol.* **2024**, *6*, 216–222. [CrossRef]
12. Bartolome, G.J.C.; Tayo, L.L. Decolorization of Methyl Orange using a Double-chamber Microbial Fuel Cell with the Use of Soil Microorganisms. *IOP Conf. Ser. Earth Environ. Sci.* **2020**, *563*, 012007. [CrossRef]
13. Naaz, T.; Sharma, K.; Roy, A.; Singh Mathuriya, A.; Yadav, V.; Pandit, S.; Hasan, M.; Anand, J.; Joshi, S.; Sharma, R. Simultaneous microbial electrochemical degradation of methyl orange and bioelectricity generation using coculture as anode inoculum in a microbial fuel cell. *Food Chem. Toxicol.* **2023**, *181*, 114058. [CrossRef] [PubMed]
14. Guo, D.; Fu, Q.; Wang, X.; Li, L.; Xu, X.; An, X. Natural tea polyphenol functionalized graphene anode for simultaneous power production and degradation of methyl orange dye in microbial fuel cells. *RSC Adv.* **2024**, *14*, 14847–14856. [CrossRef] [PubMed]
15. Huang, W.; Chen, J.; Hu, Y.; Chen, J.; Sun, J.; Zhang, L. Enhanced simultaneous decolorization of azo dye and electricity generation in microbial fuel cell (MFC) with redox mediator modified anode. *Int. J. Hydrogen Energy* **2017**, *42*, 2349–2359. [CrossRef]
16. Chacko, A.; Akhila, U.; Noori, M.T.; Rajesh, P.P. Effect of heat pretreatment of anodic inoculum in microbial fuel cell for enhanced methyl orange dye degradation and electricity generation. *Sustain. Energy Technol. Assess.* **2025**, *82*, 104525. [CrossRef]
17. APHA. *Standard Methods for the Examination of Water and Wastewater*, 21st ed.; American Public Health Association: Washington, DC, USA, 2005.
18. Logan, B.E.; Hamelers, B.; Rozendal, R.; Schröder, U.; Keller, J.; Freguia, S.; Aelterman, P.; Verstraete, W.; Rabaey, K. Microbial fuel cells: Methodology and technology. *Environ. Sci. Technol.* **2006**, *40*, 5181–5192. [CrossRef] [PubMed]
19. Joksimović, K.; Kodranov, I.; Randjelović, D.; Slavković Beškoski, L.; Radulović, J.; Ljević, M.; Manojlović, D.; Beškoski, V.P. Microbial fuel cells as an electrical energy source for degradation followed by decolorization of Reactive Black 5 azo dye. *Bioelectrochemistry* **2022**, *145*, 108088. [CrossRef] [PubMed]
20. Mittal, Y.; Dash, S.; Srivastava, P.; Mishra, P.M.; Aminabhavi, T.M.; Yadav, A.K. Azo dye containing wastewater treatment in earthen membrane based unplanted two chambered constructed wetlands-microbial fuel cells: A new design for enhanced performance. *Chem. Eng. J.* **2022**, *427*, 131856. [CrossRef]
21. Khalik, W.F.; Ho, L.N.; Ong, S.A.; Voon, C.H.; Wong, Y.S.; Yusoff, N.A.; Lee, S.L.; Yusuf, S.Y. Optimization of degradation of Reactive Black 5 (RB5) and electricity generation in solar photocatalytic fuel cell system. *Chemosphere* **2017**, *184*, 112–119. [CrossRef] [PubMed]
22. Mani, P.; Fidal, V.T.; Bowman, K.; Breheny, M.; Chandra, T.S.; Keshavarz, T.; Kyazze, G. Degradation of Azo Dye (Acid Orange 7) in a Microbial Fuel Cell: Comparison Between Anodic Microbial-Mediated Reduction and Cathodic Laccase-Mediated Oxidation. *Front. Energy Res.* **2019**, *7*, 101. [CrossRef]
23. Hong, Y.; Call, D.F.; Werner, C.M.; Logan, B.E. Adaptation to high current using low external resistances eliminates power overshoot in microbial fuel cells. *Biosens. Bioelectron.* **2011**, *28*, 71–76. [CrossRef] [PubMed]
24. Khan, M.D.; Abdulateif, H.; Ismail, I.M.; Sabir, S.; Khan, M.Z. Bioelectricity generation and bioremediation of an azo-dye in a microbial fuel cell coupled activated sludge process. *PLoS ONE* **2015**, *10*, e0138448. [CrossRef] [PubMed]
25. Khan, M.D.; Li, D.; Tabraiz, S.; Shamurad, B.; Scott, K.; Khan, M.Z.; Yu, E.H. Integrated air cathode microbial fuel cell-aerobic bioreactor set-up for enhanced bioelectrodegradation of azo dye Acid Blue 29. *Sci. Total Environ.* **2021**, *756*, 143752. [CrossRef] [PubMed]
26. Shahi, A.; Velayudhaperumal Chellam, P.; Verma, A.; Singh, R.S. A comparative study on the performance of microbial fuel cell for the treatment of reactive orange 16 dye using mixed and pure bacterial species and its optimization using response surface methodology. *Sustain. Energy Technol. Assess.* **2021**, *48*, 101667. [CrossRef]

Disclaimer/Publisher's Note: The statements, opinions and data contained in all publications are solely those of the individual author(s) and contributor(s) and not of MDPI and/or the editor(s). MDPI and/or the editor(s) disclaim responsibility for any injury to people or property resulting from any ideas, methods, instructions or products referred to in the content.